2444–2452 *Nucleic Acids Research, 2010, Vol. 38, No. 7* *Published online 21 January 2010*
doi:10.1093/nar/gkp1206

The DNA binding and 3′-end preferential activity of human tyrosyl-DNA phosphodiesterase

Thomas S. Dexheimer[1], Andrew G. Stephen[2], Matthew J. Fivash[3], Robert J. Fisher[2] and Yves Pommier[1,*]

[1]Laboratory of Molecular Pharmacology, Center for Cancer Research, National Cancer Institute, National Institutes of Health, 37 Convent Drive, Building 37, Room 5068, Bethesda, MD 20892-4255, [2]Protein Chemistry Laboratory, Advanced Technology Program, SAIC-Frederick Inc. and [3]Data Management Systems Inc., NCI-Frederick, Frederick, MD 21702, USA

Received September 30, 2009; Revised December 12, 2009; Accepted December 14, 2009

ABSTRACT

Human tyrosyl-DNA phosphodiesterase (Tdp1) processes 3′-blocking lesions, predominantly 3′-phosphotyrosyl bonds resulting from the trapping of topoisomerase I (Top1) cleavage complexes. The controversial ability of yeast Tdp1 to hydrolyze 5′-phosphotyrosyl linkage between topoisomerase II (Top2) and DNA raises the question whether human Tdp1 possesses 5′-end processing activity. Here we characterize the end-binding and cleavage preference of human Tdp1 using single-stranded 5′- and 3′-fluorescein-labeled oligonucleotides. We establish 3′-fluorescein as an efficient surrogate substrate for human Tdp1, provided it is attached to the DNA by a phosphodiester (but not a phosphorothioate) linkage. We demonstrate that human Tdp1 lacks the ability to hydrolyze a phosphodiester linked 5′-fluorescein. Using both fluorescence anisotropy and time-resolved fluorescence quenching techniques, we also show the preferential binding of human Tdp1 to the 3′-end. However, DNA binding competition experiments indicate that human Tdp1 binding is dependent on DNA length rather than number of DNA ends. Lastly, using surface plasmon resonance, we show that human Tdp1 selectively binds the 3′-end of DNA. Together, our results suggest human Tdp1 may act using a scanning mechanism, in which Tdp1 bind non-specifically upstream of a 3′-blocking lesion and is preferentially stabilized at 3′-DNA ends corresponding to its site of action.

INTRODUCTION

DNA strand breaks caused by exogenous and endogenous sources often contain blocking terminal groups with abnormal structures that must be initially removed by DNA end-processing enzymes prior to their repair by DNA polymerases and sealing by DNA ligases. One such DNA repair enzyme, tyrosyl-DNA phosphodiesterase (Tdp1), catalyzes the hydrolysis of a variety of 3′-lesions from DNA resulting in a 3′-phosphate product [for review, see ref. (1)]. Tdp1 efficiently processes 3′-phosphotyrosyl linkages, which arise from abortive topoisomerase I (Top1)–DNA cleavage complexes (2–4). Other physiological Tdp1 substrates include 3′-phosphoglycolates (5) and 3′-abasic sites (6). In addition, Tdp1 possesses a 3′-nucleosidase activity in which a single nucleoside is removed from 3′-hydroxy terminated ribo- and deoxyribonucleosides (6). This non-processive single-base excision is explained by the fact that 3′-phosphate terminated ends are non-hydrolyzable Tdp1 substrates (6). Such 3′-phosphate ends generated by Tdp1 are efficiently removed by polynucleotide kinase 3′-phosphatase (PNKP) to produce a 3′-hydroxyl, which can then be processed further and repaired by DNA ligases and polymerases (7–9).

The physiological importance of Tdp1 in DNA repair stems from the observation that a mutation in the human *TDP1* gene, which results in an active site histidine to arginine mutation (H493R), has been associated with the rare neurodegenerative disorder spinocerebellar ataxia with axonal neuropathy (SCAN1) (10). Lymphoblastoid cell lines from SCAN1 patients are hypersensitive to both camptothecin (CPT) and oxidative stress (11–14). In addition, the recent generation of Tdp1 knockout mice has further established the involvement of Tdp1 in the repair of both Top1–DNA adducts and oxidative DNA

*To whom correspondence should be addressed. Tel: 301 496 5944; Fax: 301 402 0752; Email: pommier@nih.gov

damage based on the sensitivity of cells derived from Tdp1$^{-/-}$ mice to CPT and bleomycin or hydrogen peroxide, respectively (15,16).

Several non-physiological Tdp1 substrates have also been identified including a 3′-biotin linked adduct (6) and a fluorescent 3′-(4-methylumbelliferone) reporter molecule (17) as well as two 3′-phosphotyrosine analogs, 3′-(4-nitro)phenol and 3′-(4-methyl)phenol (17). These types of substrates have proven useful for measuring Tdp1 activity and screening for Tdp1 inhibitors (17–19). In addition, such substrates have a decisive advantage over the naturally occurring Tdp1 substrates in that they are more cost-effective.

Discrepancies still remain concerning the 5′-end processing activity of Tdp1. While Yang *et al.* initially showed that partially purified yeast Tdp1 was unable to process 5′-tyrosine-containing oligonucleotides (2), subsequent studies have suggested that recombinant yeast Tdp1 can remove 5′-phosphotyrosyl peptides from DNA or more specifically topoisomerase II (Top2)-related DNA adducts (20). Those biochemical results were supported by the hypersensitivity of yeast *tdp1* mutants overexpressing Top2 to the clinically used Top2 inhibitor, etoposide (20). It has also been shown that enhanced expression of human Tdp1 in cultured cells effectively decreases etoposide-induced Top2-mediated DNA damage (21). The crystal structures of the yeast (22) and human (23) Tdp1 proteins show minimal differences in active site architecture in spite of large differences in amino acid composition, suggesting similar catalytic mechanisms. However, biochemical data have been lacking to question the 5′-end binding and processing associated with human Tdp1.

To better understand what determines the 3′-end-specific recognition and processing activities of human Tdp1, we have examined the DNA binding and cleavage properties of human Tdp1 using 5′- and 3′-fluorescein-labeled oligonucleotides. We have also analyzed for the first time the binding of human Tdp1 to non-hydrolyzable 3′-ends containing a 3′-phosphate or a 3′-phosphorothioate-linked fluorescein.

MATERIALS AND METHODS

Materials

All DNA oligonucleotides were synthesized by Integrated DNA Technologies (Coralville, IA, USA) with the exception of those containing a fluorescein attached via a phosphorothioate linkage, which were synthesized by Sigma-Genosys (St Louis, MO, USA). T4 polynucleotide 3′-phosphatase (PNK) and the 3′-phosphatase minus mutant T4 PNK [PNK(−)] were purchased from New England BioLabs (Cambridge, MA, USA). Terminal deoxynucleotidyl transferase (TdT) was purchased from Calbiochem (La Jolla, CA, USA).

Expression and purification of Tdp1

Human Tdp1 was expressed in *Escherichia coli* BL21 (DE3) cells and purified as described earlier (18).

Preparation of radiolabeled oligonucleotides

DNA oligonucleotides were either 5′-end labeled using PNK and [γ-^{32}P] ATP or 3′-end labeled using TdT and [α-^{32}P] cordycepin-5′-triphosphate, respectively. Unincorporated radioactive nucleotides were removed using a mini Quick Spin Oligo column (Roche Diagnostics, Indianapolis, IN, USA).

Tdp1 and PNK enzymatic assays

One nanomolar of ^{32}P-labeled oligonucleotide substrate in a 10 µl reaction volume was incubated with the indicated concentrations of recombinant Tdp1 for 30 min at 25°C in a buffer containing 50 mM Tris–HCl (pH 7.5), 25 mM KCl and 2 mM EDTA. In reactions containing PNK or PNK(−), the reaction buffer was supplemented with 10 mM $MgCl_2$. Reactions were terminated by the addition of two volumes of gel loading buffer [96% (v/v) formamide, 10 mM EDTA, 1% (w/v) xylene cyanol and 1% (w/v) bromphenol blue]. The samples were subsequently heated to 95°C for 5 min and subjected to 20% sequencing gel electrophoresis. Imaging was performed using the Typhoon 8600.

Fluorescence anisotropy

Equilibrium binding of Tdp1 to fluorescein (6-FAM)-labeled oligonucleotides was monitored by fluorescence anisotropy using previously developed methods (24). Briefly, serial dilutions of recombinant Tdp1 were mixed with 10 nM of fluorescein-labeled oligonucleotides (Table 1) in a binding buffer containing 50 mM Tris–HCl (pH 7.5), 25 mM KCl and 2 mM EDTA in a final volume of 50 µl. Aliquots (40 µl) were transferred into 384-well Costar polypropylene plates (Corning, NY, USA) and read using a Tecan Ultra plate reader (Durham, NC, USA) with excitation and emission wavelengths of 485 and 535 nm, respectively.

Table 1. Sequence, structure, and calculated dissociation constants (K_D) of oligonucleotides used in this study

Name	Length (nt)	Sequence (5′–3′)	K_D (nM)[a]	95% CI (nM)
14**Y**	14	GATCTAAAAGACTT-**Y**	NA	NA
14**F**	14	GATCTAAAAGACTT-**F**	NA	NA
F14	14	**F**-GATCTAAAAGACTT	76.9	66.2–87.5
F14p	14	**F**-GATCTAAAAGACTTp	34.1	26.8–41.4
14p	14	GATCTAAAAGACTTp	NA	NA
15**F**	15	GATCTAAAAGACTTG-**F**	NA	NA
15(pS)**F**	15	GATCTAAAAGACTTG(pS)-**F**	2.4	1.3–3.4
F15	15	**F**-GATCTAAAAGACTTG	39.2	31.9–46.5
F(pS)15	15	**F**-(pS)GATCTAAAAGACTTG	26.3	22.6–30.0
p14**B**	14	pGATCTAAAAGACTT-**B**	NA	NA
B14p	14	**B**-GATCTAAAAGACTTp	57.0	NA
50p	50	AAGATCTAAAAGACTTAAG GATCTAAAAGACTTGAAG ATCTAAAAGACTTp	NA	NA

Y represents the tyrosyl chemical group (Figure 1A); **F** represents the 6-FAM chemical group (Figure 1A); **B** represents the biotin chemical group; p represents the terminal phosphate; (pS) represents the phosphorothioate linkage; NA, not applicable.
[a]See 'Materials and Methods' section for K_D calculations.

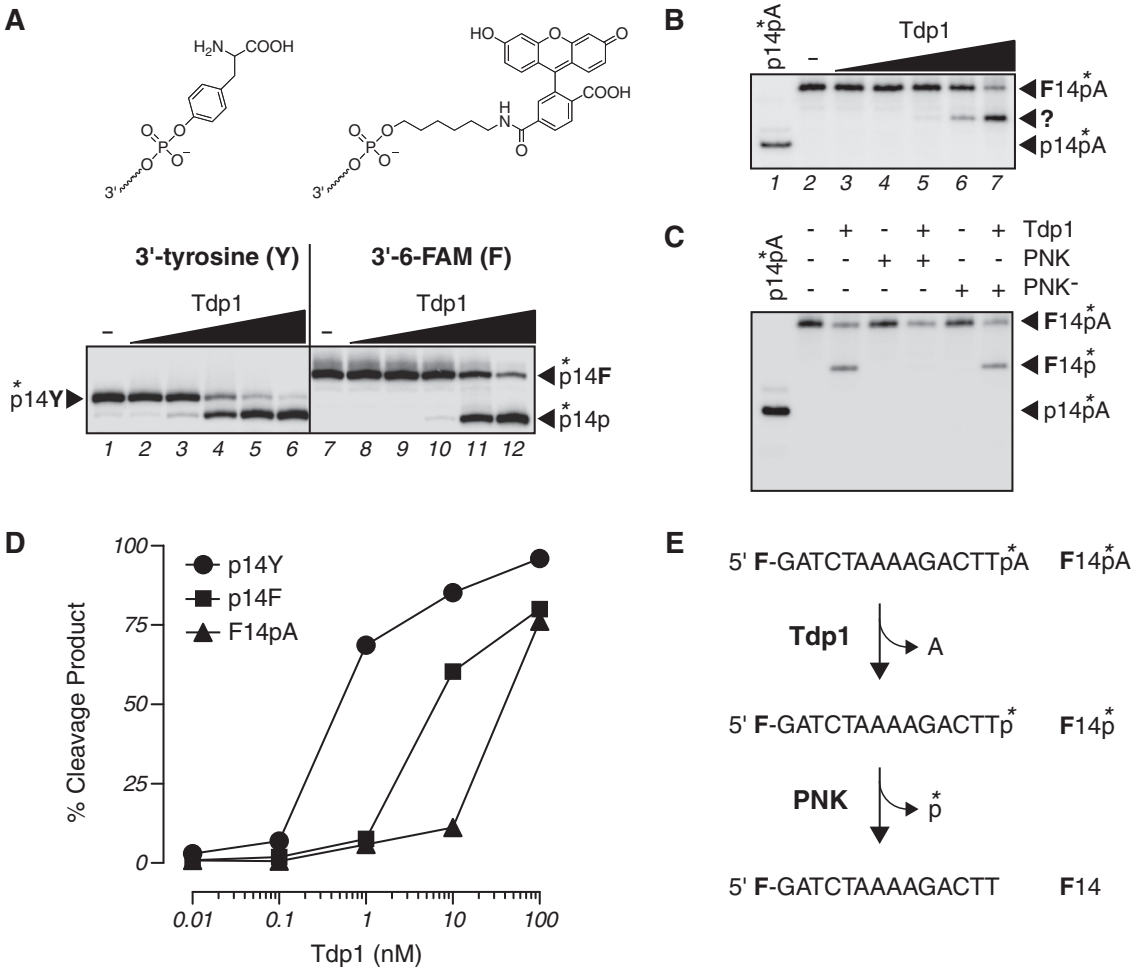

Figure 1. Processing of fluorescein-labeled oligonucleotides by recombinant human Tdp1. (**A**) Representative denaturing PAGE gel showing Tdp1-mediated conversion of 5′-end radiolabeled 14-mer oligonucleotides containing a 3′-tyrosine (p14**Y**) or 3′-fluorescein (p14**F**) to a 3′-phosphate product (p14p). The chemical structures of the 3′-tyrosine and 3′-6-FAM are shown above the gel. (**B**) Representative denaturing PAGE gel showing the generation of an unknown product (indicated by *question mark*) from Tdp1 cleavage of a 3′-end radiolabeled 14-mer oligonucleotide containing a 5′-fluorescien (**F**14pA). Tdp1 concentrations in (A) and (B) are as follows: 0.01 nM (lanes 2 and 8), 0.1 nM (lanes 3 and 9), 1 nM (lanes 4 and 10), 10 nM (lanes 5 and 11) and 100 nM (lanes 6 and 12). (**C**) 3′-end processing of the **F**14pA oligonucleotide [from (**B**)] by the combinations of Tdp1 (100 nM) and wild-type T4 PNK [PNK (1 unit), lane 5] or Tdp1 and 3′-phosphatase-minus mutant T4 PNK [PNK$^-$ (1 unit), lane 7]. (**D**) 3′-end processing of the different substrates. (**E**) Schematic illustrating the substrates and products of the sequential action of Tdp1 and PNK on the **F**14pA oligonucleotide. In all instances the asterisk indicates the ^{32}P-labeled phosphate.

Fluorescence anisotropy competition

A constant concentration of **F**14p (10 nM) was mixed with 2-fold serial dilutions of unlabeled competitor oligonucleotide in 50 mM Tris–HCl (pH 7.5), 25 mM KCl, 2 mM EDTA and placed in a 96-well Costar polypropylene plates (Corning). A constant concentration of Tdp1 (100 nM) was then added to a final volume of 50 µl and incubated at room temperature for 20 min. Aliquots (40 µl) were transferred into 384-well Costar polypropylene plates (Corning) and read using a Tecan Ultra plate reader (Durham) with excitation and emission wavelengths of 485 and 535 nm, respectively.

Fluorescence anisotropy data analysis

Equilibrium dissociation constants (K_D) were estimated from the anisotropy in three steps. First, the total intensity of the fluorophore was examined and a correction parameter, R, was estimated (25). Next, an equation relating fractional binding (f_B) and anisotropy was selected [Equation (1)],

$$\text{Anisotropy} = \frac{f_B r_B R + r_F(1 - f_B)}{f_B R - f_B + 1} \quad \mathbf{1}$$

where f_B is fractional binding; r_B is anisotropy signal of saturated binding; r_F is anisotropy signal of no binding and R is ratio of maximum and minimum total fluorescence intensity.

Finally, the fractional binding model is fit to the anisotropy signal using a nonlinear least squares algorithm. For this, the simple Langmuir model was selected [Equation (2)], where K_D refers to the dissociation constant.

$$f_B = \frac{[\text{Tdp1}_{\text{free}}][\text{DNA}_{\text{free}}]}{K_D[\text{DNA}_{\text{total}}]} \quad \mathbf{2}$$

Equations (1) and (2) are combined and solved numerically. The concentration of DNA_{free} and $Tdp1_{free}$ were solved numerically using a conservation law. The system is then fit to experimental anisotropy data using a non-linear regression operator based on a Marquardt compromise. When the K_D value is small relative to the concentration titration range, the binding may be assumed to be stoichiometric. In this case, a plot of the molar ratio of the Tdp1 and DNA versus fractional binding will achieve half saturation binding at a ratio of unity. This is checked when the DNA binds tight enough for this test to be completed.

Time resolved fluorescence

Fluorescence lifetimes were measured time-correlated single-photon counting using a PicoQuant FluoTime200 instrument. The excitation wavelength was 470 nm with a repetition rate of 10 MHz. The emission was collected at a wavelength of 535 nm through a 0.5 nm band pass under magic angle conditions. The instrument response signal was measured with a scattering solution of Ludox. All measurements were performed at ambient temperature. Fluorescein-labeled oligonucleotides were prepared in 50 mM Tris–HCl (pH 7.5), 25 mM KCl and 2 mM EDTA at a concentration of 150 nM. Recombinant Tdp1 was added (37.5–450 nM) to each oligonucleotide and the intensity decay curve was recorded. For each titration the decay curves were fit globally using the FluoFit software (PicoQuant) using a bi-exponential function. The quality of the fits were evaluated by the reduced chi-squared and randomness of the residuals.

Surface plasmon resonance binding assays

Surface plasmon resonance (SPR) binding experiments were performed on a Biacore 2000 instrument (GE, Piscataway, NJ, USA). Neutravidin was coupled to the carboxymethylated dextran surface of a CM5 sensor chip (GE, Piscataway, NJ, USA) using standard amine coupling chemistry. In brief, the surface was activated with 0.1 M N-hydroxysuccinimide and 0.4 M N-ethyl-N′-(3-dimethylaminopropyl) carbodiimide at a flow rate of 20 µl/min. Neutravidin was diluted to 200 µg/ml in 10 mM sodium acetate (pH 4.5) and injected until a density of ~1800 RU was attached. Activated amine groups were quenched with an injection of 1 M ethanolamine (pH 8.0). 5′- and 3′-biotinylated DNA oligonucleotides (see **B**14p and p14**B** in Table 1) were immobilized to the neutravidin-coated sensor chips at 37 and 28 RU, respectively. Recombinant Tdp1 was diluted in running buffer [20 mM HEPES (pH 7.5), 150 mM NaCl, 2 mM EDTA, 0.05% (w/v) Tween-20, 5 mg/ml carboxymethyl dextran, 0.05% (w/v) polyethylene glycol 20 000] in nine successive 2-fold dilutions from 500 nM and injected over the immobilized oligonucleotides for 1 min at 20 ml/min at 25°C. At the end of the injection, Tdp1-oligonucleotide complexes were allowed to dissociate for 3 min. A 30 s pulse of 1 M NaCl removed any material that remained bound to the surface. Each cycle of Tdp1 injection was followed by a running buffer cycle for referencing purposes. To ensure the integrity of the oligonucleotide surface was not compromised by Tdp1 binding, five injections of 50 nM HIV-1 nucleocapsid protein were made through the course of the experiment. The binding kinetics of Tdp1 could not be fit with a simple Langmuir binding model. However, the equilibrium binding response was fit with a Langmuir binding model using BiaEvaluation software.

RESULTS

Human Tdp1 can remove fluorescein from the 3′-end, but not the 5′-end of DNA

Based on the structural diversity of substrates that are cleaved by Tdp1 (1,5,6), we reasoned that a fluorescein molecule could also serve as a convenient and quantitative probe to investigate the DNA binding and processing of human Tdp1. To address the end-specific cleavage (3′ versus 5′) of human Tdp1, 14-mer oligonucleotide conjugates were synthesized containing the fluorescein derivative, 6-FAM (chemical structure shown in Figure 1A), attached via the terminal phosphodiester at the 3′- or 5′-end of the oligonucleotide (14**F** and **F**14 in Table 1, respectively). As expected, the 3′-fluorescein-phosphodiester bond of the 14**F** oligonucleotide was hydrolyzed by human Tdp1 to generate the 3′-phosphate-terminated 14-mer product (Figure 1A). However, this reaction was less efficient than the 3′-phosphotyrosine substrate (14**Y** in Table 1) (Figure 1A and D).

Having established that 3′-fluorescein is a substrate for Tdp1, we tested whether Tdp1 could also process 5′-fluorescein-DNA (**F**14). Figure 1B shows that a single cleavage product was observed with the **F**14 oligonucleotide. However, this product exhibited a reduced migration relative to the 5′-phosphate-terminated marker (Figure 1B), suggesting that Tdp1 is unable to simply cleave the fluorescein adduct linked to the 5′-end of DNA. Given that the TdT-mediated 3′-end ^{32}P-radiolabeling of the **F**14 oligonucleotide leads to the addition of a 3′-terminal 3′-deoxyadenosine (cordycepin), we considered the possibility that the detected cleavage product may be a consequence of the 3′-nucleosidase activity of Tdp1. To establish the occurrence of this 3′-nucleolytic product, we utilized the 3′-phosphatase activity of polynucleotide kinase from bacteriophage T4 (PNK) to show that the product of the Tdp1 reaction contained a 3′-terminal ^{32}P-radiolabel. As shown in Figure 1C, the combination of Tdp1 and PNK resulted in the disappearance of the product (compare lanes 3 and 5), which indicates the removal of the 3′-deoxynucleoside by Tdp1 followed by removal of the resulting 3′-terminal ^{32}P-radiolabel by PNK (Figure 1E). This result was further corroborated in control reactions, which employed a 3′-phosphatase-minus T4 PNK mutant [PNK$^-$] (see lane 7). Similar results were obtained using a 5′-biotin-DNA substrate (data not shown). Taken together, these results demonstrate that human Tdp1 can hydrolyze a 3′-terminal phosphodiester-linked fluorescein or nucleoside leading to a 3′-phosphate DNA end under

conditions where it has no detectable activity towards a 5′-terminal-phosphodiester-linked fluorescein.

Fluorescence anisotropy analysis of binding of human Tdp1 to fluorescein-labeled oligonucleotides

To characterize the DNA binding properties of human Tdp1 depending on the presence of fluorescein at the 5′- or 3′-end of the substrate, we measured changes in the anisotropy of fluorescein-labeled oligonucleotides upon titration with Tdp1. Fluorescence anisotropy is a spectroscopic technique that monitors macromolecular associations predominantly through changes in the rotational motion of fluorescent molecules (25). As the molecular weight of the fluorophore increases, due to Tdp1–DNA binding, the rotational freedom of the DNA is reduced, leading to an increase in anisotropy (i.e. retention of polarization). This is illustrated schematically in Figure 2A.

For these experiments, we employed the two fluorescein-labeled oligonucleotides previously employed in the enzymatic activity assays (14**F** and **F**14) as well as an additional 5′-fluorescein-labeled oligonucleotide containing a 3′-phosphate (Table 1, **F**14p), known not to be hydrolyzed by Tdp1 (6). Figure 2B depicts the fluorescent anisotropy with increasing concentration of Tdp1. No increase in anisotropy was observed with the 3′-labeled oligonucleotide (14**F**), which was anticipated, given that Tdp1 hydrolyzes the 3′-fluorescein (Figure 1A). More interestingly, we detected a concentration-dependent enhancement in anisotropy for both 5′-labeled oligonucleotides (**F**14 and **F**14p). Based on calculated K_D values (Table 1), Tdp1 bound with an ~3-fold higher affinity to **F**14p than it did to **F**14. There are two possible explanations for this difference. First, Tdp1 may bind better to a 3′-phosphate as compared to a 3′-hydroxyl; or second, Tdp1 may have a higher binding affinity for longer DNA sequences *in vitro*. The latter is based on the fact that Tdp1 can hydrolyze 3′-hydroxyl ends (Figure 1B), which would result in a one base shorter **F**13p oligonucleotide product. Consistent with that explanation, previous studies have shown that Tdp1 is more effective at processing DNA-peptide substrates with a longer DNA component (4). Further support for the DNA length dependent binding of human Tdp1 is shown in Figure 2C, wherein Tdp1 shows a roughly

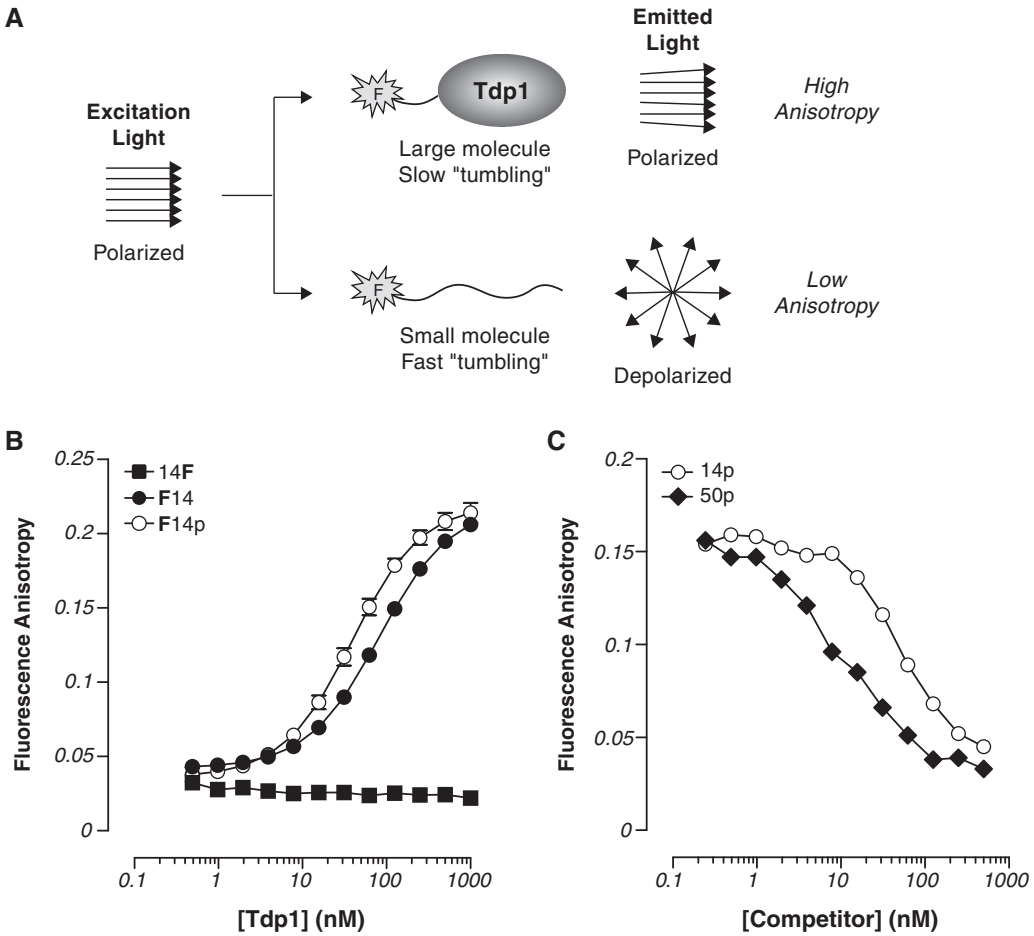

Figure 2. Equilibrium binding of recombinant human Tdp1 to fluorescein-labeled oligonucleotides using fluorescence anisotropy. (**A**) Schematic diagram showing the principle of fluorescence anisotropy. (**B**) Fluorescence anisotropic signal for 14**F** (filled squares), **F**14 (filled circles) and **F**14p (open circles) as a function of Tdp1 concentration. Each point of the graph represents the mean ($n = 3$) ±95% confidence interval (error bars). (**C**) Analysis of the competition between oligonucleotides in solution using fluorescence anisotropy. Representative plots of Tdp1 binding competition between **F**14p and unlabeled 14p (open circles) or 50p (filled diamonds).

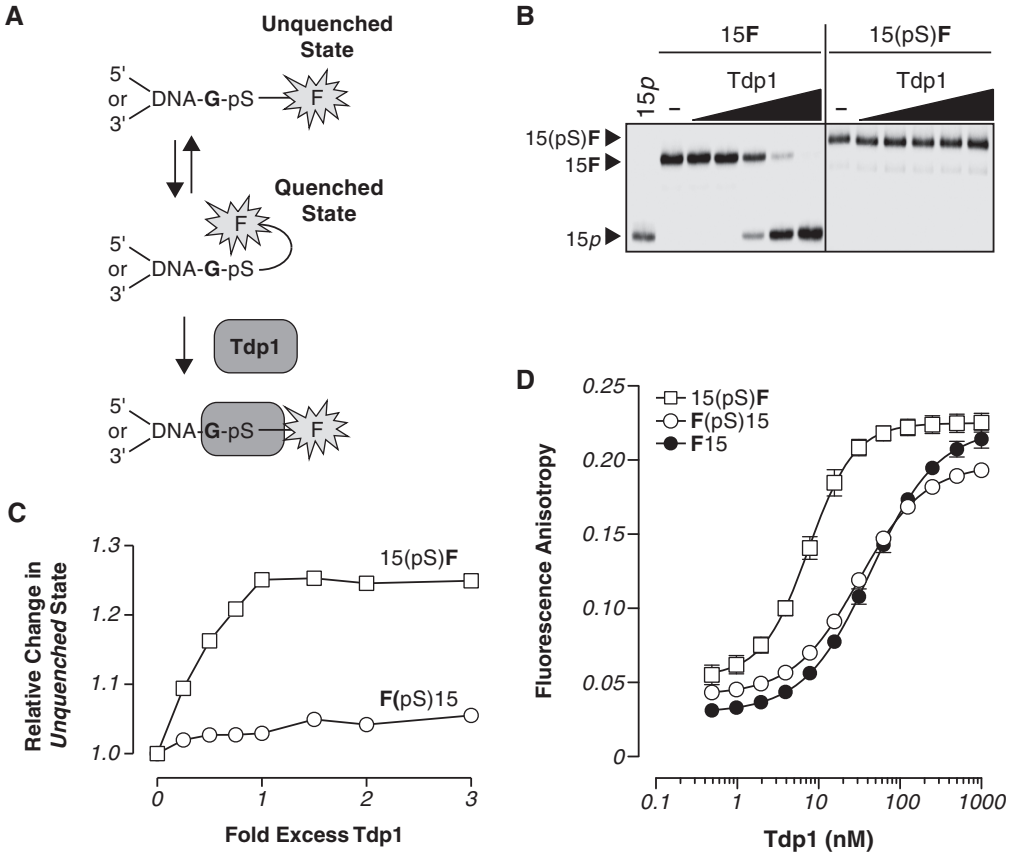

Figure 3. Binding and processing of phosphorothioate-linked fluorescein containing oligonucleotides by recombinant human Tdp1. (**A**) Simplified representation of the quenched and unquenched states of the terminal fluorescein in the absence and presence of Tdp1. (**B**) Representative denaturing PAGE gel showing the hydrolyzability and non-hydrolyzability of a 3′-fluorescein attached via a phosphodiester linkage (15**F**) and phosphorothioate linkage [15(pS)**F**] by Tdp1, respectively. (**C**) Graphical representation of the relative change in the fluorescence lifetime of the unquenched state for **F**(pS)15 (filled circles) and 15(pS)**F** (open circles) as a function of Tdp1 concentration. (**D**) Fluorescence anisotropic signal for 15**F** (filled squares), 15(pS)**F** (open squares), **F**15 (filled circles) and **F**(pS)15 (open circles) as a function of Tdp1 concentration. Each point on the graph represents the mean ($n = 3$) ±95% confidence interval (error bars).

10-fold higher affinity for a 50-mer 3′-phosphate containing oligonucleotide as compared to a 14p oligonucleotide using a fluorescence anisotropy competition assay. These results also suggest that Tdp1 does not have to initially bind to the 3′-end of the DNA. If Tdp1 was directly binding the 3′-end of the DNA, then one would expect the binding curves to be indistinguishable given that both oligonucleotides have a single 3′-end available for binding. Thus, these results imply that Tdp1 may initially interact electrostatically with the DNA prior to reaching its site of action (i.e. the 3′-end).

3′-end specific binding of human Tdp1 to a non-hydrolyzable, phosphorothioate-linked 3′-fluorescein-containing oligonucleotide

Previous studies have demonstrated that guanosine residues have the propensity to quench the fluorescence intensity of fluorescein-oligonucleotide conjugates (25–7). More specifically, it has been shown that the time-resolved fluorescence decay of a fluorescein located proximal to a guanosine residue in a single-stranded oligonucleotide is fitted to a bi-exponential function with two apparent decay lifetimes (27). This indicates that the fluorescein is found in two distinct conformations. The longer lifetime corresponds to an unquenched state or direct excitation of the fluorescein, whereas the shorter lifetime refers to a quenched state or rapid charge transfer reaction between the fluorescein and the guanosine residue (Figure 3A). Furthermore, the bi-exponential fit allows for determination of the relative abundance or amplitude of the two decay lifetimes.

To assess the end-specific binding of human Tdp1 using the aforementioned guanosine quenching method, we designed two oligonucleotides wherein a guanosine base was placed adjacent to the 5′- or 3′-terminal fluorescein. We envisioned that if human Tdp1 possesses a 3′-end specific binding activity, then we would observe a decrease in quenching, as Tdp1 would occlude the 3′-fluorescein from interacting with the adjacent guanosine residue (Figure 3A).However, prior to testing our hypothesis a non-hydrolyzable Tdp1 substrate had to be developed given that Tdp1 readily removes a phosphodiester-linked 3′-fluorescein (Figure 1A). Phosphorothioate linkages are commonly used to reduce oligonucleotide sensitivity toward nucleases. In addition, phosphorothioate modifications have been used to study

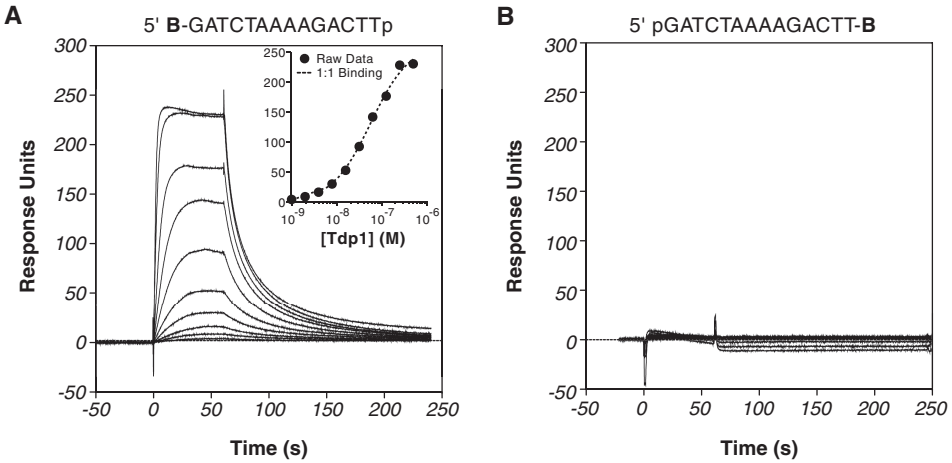

Figure 4. Differential binding of recombinant human Tdp1 to 3′- and 5′-phosphate terminated oligonucleotides using SPR. SPR sensorgrams showing the interaction of Tdp1 with the (**A**) **B**14p oligonucleotide and (**B**) p14**B** oligonucleotide (see sequences above). Nine successive 2-fold dilutions of Tdp1 from 500 nM were tested for each oligonucleotide. The inset in (A) shows the equilibrium binding of Tdp1 to **B**14p fitted to the 1:1 Langmuir binding model.

the action of other phospholipase D enzymes (28,29). Therefore, we reasoned that attaching the 3′-fluorescein via a phosphorothioate linkage might result in a non-hydrolyzable Tdp1 substrate, which subsequently could be exploited for end-specific DNA binding studies.

As shown in Figure 3B, the phosphorothioate-linked 3′-fluorescein [15(pS)**F**] is resistant to Tdp1 hydrolysis under conditions where Tdp1 is able to remove phosphodiester-linked 3′-fluorescein (15**F**). These results enabled us to use the phosphorothioate-linked 3′- and 5′-fluorescein-labeled oligonucleotides [15(pS)**F** and **F**(pS)15 in Table 1, respectively] as probes for the time-resolved fluorescence quenching studies. We observed a concentration-dependent increase in the unquenched state of the 3′-fluorescein upon titration with recombinant human Tdp1. By contrast only minimally changes were discerned for the 5′-fluorescein (Figure 3C, lower curve). In addition, we found that the binding of Tdp1 to the non-hydrolyzable, 3′-fluorescein-containing oligonucleotide reached a plateau at a 1:1 molar ratio. These results provide additional data on the distribution of different species in solution and are consistent with the 3′-end DNA binding of human Tdp1.

Fluorescence anisotropy was then used to quantify the binding of human Tdp1 to the fluorescent probes. The attachment of 5′-fluorescein via a phosphodiester or phosphorothioate linkage produced similar Tdp1 binding [compare **F**15 and **F**(pS)15 in Figure 3D), which was expected given that both oligonucleotides have identical 3′-termini (i.e. 3′-hydroxyl) (Table 1). Conversely, binding of Tdp1 to the non-hydrolyzable 15(pS)**F** oligonuceotide could now be detected by fluorescence anisotropy and was at least 10-fold more efficient than the 5′-fluorescein-linked oligonucleotides (Figure 3D and K_D values in Table 1). Taken together, these results suggest that unnatural 3′-adducts may create a high affinity binding site for human Tdp1.

Preferential binding of human Tdp1 to the 3′-end of DNA using SPR

To gain further evidence that human Tdp1 binds to the 3′-end of DNA, we utilized SPR wherein oligonucleotides were biotinylated at either the 5′- or 3′-end for end-specific immobilization to a neutravidin-coated sensor chip (**B**14p and p14**B** in Table 1). As shown in Figure 4A by the increase in response units from the initial baseline, Tdp1 binds with high affinity to the 5′-biotin immobilized, 3′-phosphate containing oligonucleotide (**B**14p) in a concentration-dependent manner. The Tdp1 binding kinetics to the **B**14p oligonucleotide could not be fit assuming a single association and dissociation rate constant. The complex kinetics may be due to non-specific binding of Tdp1 to the surface, kinetic heterogeneity in the Tdp1 protein sample, or transport effects. However, Tdp1 does form a stable complex with the **B**14p oligonucleotide at each Tdp1 concentration (Figure 4A). This equilibrium binding response can be fit to a Langmuir binding model assuming a 1:1 binding interaction (inset in Figure 4A) with a K_D value of 57 nM (Table 1). In contrast, SPR analysis of the oligonucleotide immobilized in the opposite orientation (p14**B**) results in a complete loss of Tdp1 DNA binding activity (Figure 4B), indicating that the interaction between the DNA and Tdp1 requires an exposed 3′-end. Given the previously described ability of Tdp1 to hydrolyze 3′-linked biotin adducts (6), it is worth noting that the maintenance of the immobilized oligonucleotides subsequent to assaying the DNA binding activity of Tdp1 was ensured based on reproducible binding of HIV nucleocapsid protein (data not shown) (24).

DISCUSSION

DNA strand breaks are a frequent source of 'blocking' DNA ends that can impede essential biological processes

(9). Tdp1 is an enzyme conserved from yeast to mammals, and which is involved in the initial processing of a subset of these DNA ends as a prerequisite for further repair (2,30). The removal of a variety of 3′-end lesions is a well-accepted enzymatic activity of both the human and yeast Tdp1 proteins. However, the 5′-processing activity of Tdp1 has been less studied. In their initial discovery of the yeast Tdp1 enzyme, Yang *et al*. (2) reported lack of an associated 5′-processing activity. Nevertheless, it has recently been suggested that yeast Tdp1 participates in the repair of Top2-mediated DNA damage (i.e. 5′-DNA–peptide adducts) ('Introduction' section) (20,21).

In this report, we utilized 3′- and 5′-fluorescein-labeled (i.e. 6-FAM) oligonucleotides as Tdp1 substrates to examine the end-specific binding and processing of human Tdp1. Initially, we demonstrate that a 3′-fluorescein is an efficient substrate for human Tdp1 (Figure 1A). It is worth noting that similar to Interthal *et al*. (6), we have not yet encountered a 3′-phosphodiester-linked chemical moiety, albeit physiological or non-physiological, that is not hydrolyzed by human Tdp1 *in vitro*. Yet, we show here that introduction of a phosphorothioate is sufficient to completely block Tdp1 enzymatic activity.

The broad 3′-end specificity of Tdp1 is not surprising given that minimal contacts beyond the terminal 3′-phosphodiester are observed in the human Tdp1 co-crystal structure bound to a DNA–Top1-derived peptide substrate mimic (31). However, this observation does not account for the differences in processing efficiency of 3′-lesions by Tdp1. For example, ~10-fold more enzyme is required to hydrolyze the 3′-fluorescein as compared to a 3′-phosphotyrosine linkage (Figure 1A and D). Moreover, a considerable excess of enzyme, ~50- and 80-fold, is needed for removal of a 3′-nucleoside (6) and a 3′-glycolate (5), respectively. Thus, additional co-crystal structures are warranted to explain the differential activity of human Tdp1 toward different 3′-adducts. Our fluorescence anisotropy studies demonstrate higher binding affinity of human Tdp1 for unnatural 3′-adducts (i.e. fluorescence) as compared to normal 3′-nucleoside (i.e. 3′-hydroxyl) or 3′-nucleotide (i.e. 3′-phosphate) containing oligonucleotides (Table 1 and Figures 2B and 3D). These results are consistent with the preferential activity of Tdp1 toward 3′-blocking adducts over physiological DNA ends.

The internal location of the 3′-phosphotyrosyl bond within a stalled full-length Top1–DNA complex is an unmanageable substrate for Tdp1 (32). Proteosomal degradation of Top1, which presumably results in enhanced access of the 3′-phosphotyrosyl bond, has been suggested for Tdp1 action *in vivo* (33). Several studies have shown that Tdp1 can hydrolyze 3′-phosphotyrosyl-linked peptides, however markedly less efficiently than a 3′-phosphotyrosine (3,4,6). Thus, the 3′-fluorescein substrate is a plausible surrogate for the physiological Tdp1 substrates: Top1 polypeptide-linked DNA, 3′-phosphoglycolates and 3′-nucleosides. In addition, 3′-phosphodiester-linked substrates, such as fluorescein and biotin (6), provide convenient ways to study Tdp1 binding and catalytic activities. Our finding that a terminal 3′-phosphorothioate-linked adducts (i.e. fluorescein) imparts resistance to Tdp1 hydrolysis may also be of use (Figure 3A).

While in agreement with the initial study from Yang *et al*. (2), but in contrast to a more recent report regarding yeast Tdp1 (20), we were unable to detect any processing of a 5′-fluorescein by human Tdp1 (Figure 1B). We extended this observation using both time-resolved fluorescence quenching (Figure 3C) and SPR (Figure 4B) to demonstrate the inability of human Tdp1 to bind DNA 5′-end. At the same time these biophysical techniques provided strong and consistent evidence for strong binding of human Tdp1 to DNA 3′-ends. The difference between the human enzyme [our results and ref. (2)] and the yeast enzyme (20) regarding 5′-ends might be due to the different substrates or specific activity of the enzymes used. We cannot exclude the possibility that 5′-peptide-DNA adducts might behave differently than the fluorescein or tyrosyl substrates, which are readily processed when placed at the 3′-end of DNA but not when they are at the 5′-end (present study). The published results in ref. (21) are challenging to explain because the processing of Top2 covalent complexes is poorly understood (34). It is not excluded that Tdp1 could play a role in processing the DNA ends following Top2 removal but without being directly involved in hydrolyzing the Top2–tyrosyl-DNA linkage.

In summary, the results presented here show converging lines of evidence that the human Tdp1 protein preferentially binds and processes the 3′-ends of DNA. The apparent lack of 5′-end processing activity of human Tdp1 is likely to be compensated by a complementary enzyme with 5′-phosphodiesterase activity. A recent report has discovered Tdp2 (TTRAP) as the enzyme that carries out the 5′-processing in human cells and plays a role in the removal of Top2–DNA adducts as well as other 5′-adducts (35).

ACKNOWLEDGEMENTS

The content of this publication does not necessarily reflect the views or policies of the Department of Health and Human Services, nor does mention of trade names, commercial products, or organizations imply endorsement by the US Government.

FUNDING

Our studies are supported by the Center for Cancer Research, National Cancer Institute, National Institutes of Health, DHHS, Bethesda, Maryland (Grant number Z01 BC 006150-19LMP). The wild-type human Tdp1 construct were generous gift from Dr H. Nash (Laboratory of Molecular Biology, National Institute of Mental Health, National Institutes of Health). This project has been funded in whole or in part with federal funds from the National Cancer Institute, National Institutes of Health, under contract HHSN261200800001E.

Conflict of interest statement. None declared.

REFERENCES

1. Dexheimer,T.S., Antony,S., Marchand,C. and Pommier,Y. (2008) Tyrosyl-DNA phosphodiesterase as a target for anticancer therapy. *Anticancer Agents Med. Chem.*, **8**, 381–389.
2. Yang,S.W., Burgin,A.B. Jr, Huizenga,B.N., Robertson,C.A., Yao,K.C. and Nash,H.A. (1996) A eukaryotic enzyme that can disjoin dead-end covalent complexes between DNA and type I topoisomerases. *Proc. Natl Acad. Sci. USA*, **93**, 11534–11539.
3. Interthal,H., Pouliot,J.J. and Champoux,J.J. (2001) The tyrosyl-DNA phosphodiesterase Tdp1 is a member of the phospholipase D superfamily. *Proc. Natl Acad. Sci. USA*, **98**, 12009–12014.
4. Debethune,L., Kohlhagen,G., Grandas,A. and Pommier,Y. (2002) Processing of nucleopeptides mimicking the topoisomerase I-DNA covalent complex by tyrosyl-DNA phosphodiesterase. *Nucleic Acids Res.*, **30**, 1198–1204.
5. Inamdar,K.V., Pouliot,J.J., Zhou,T., Lees-Miller,S.P., Rasouli-Nia,A. and Povirk,L.F. (2002) Conversion of phosphoglycolate to phosphate termini on 3′ overhangs of DNA double strand breaks by the human tyrosyl-DNA phosphodiesterase hTdp1. *J. Biol. Chem.*, **277**, 27162–27168.
6. Interthal,H., Chen,H.J. and Champoux,J.J. (2005) Human Tdp1 cleaves a broad spectrum of substrates, including phosphoamide linkages. *J. Biol. Chem.*, **280**, 36518–36528.
7. Karimi-Busheri,F., Daly,G., Robins,P., Canas,B., Pappin,D.J., Sgouros,J., Miller,G.G., Fakhrai,H., Davis,E.M., Le Beau,M.M. *et al.* (1999) Molecular characterization of a human DNA kinase. *J. Biol. Chem.*, **274**, 24187–24194.
8. Karimi-Busheri,F., Lee,J., Tomkinson,A.E. and Weinfeld,M. (1998) Repair of DNA strand gaps and nicks containing 3′-phosphate and 5′-hydroxyl termini by purified mammalian enzymes. *Nucleic Acids Res.*, **26**, 4395–4400.
9. Wilson,D.M. 3rd (2007) Processing of nonconventional DNA strand break ends. *Environ. Mol. Mutagen.*, **48**, 772–782.
10. Takashima,H., Boerkoel,C.F., John,J., Saifi,G.M., Salih,M.A., Armstrong,D., Mao,Y., Quiocho,F.A., Roa,B.B., Nakagawa,M. *et al.* (2002) Mutation of TDP1, encoding a topoisomerase I-dependent DNA damage repair enzyme, in spinocerebellar ataxia with axonal neuropathy. *Nat. Genet.*, **32**, 267–272.
11. El-Khamisy,S.F., Hartsuiker,E. and Caldecott,K.W. (2007) TDP1 facilitates repair of ionizing radiation-induced DNA single-strand breaks. *DNA Repair*, **6**, 1485–1495.
12. El-Khamisy,S.F., Saifi,G.M., Weinfeld,M., Johansson,F., Helleday,T., Lupski,J.R. and Caldecott,K.W. (2005) Defective DNA single-strand break repair in spinocerebellar ataxia with axonal neuropathy-1. *Nature*, **434**, 108–113.
13. Interthal,H., Chen,H.J., Kehl-Fie,T.E., Zotzmann,J., Leppard,J.B. and Champoux,J.J. (2005) SCAN1 mutant Tdp1 accumulates the enzyme–DNA intermediate and causes camptothecin hypersensitivity. *EMBO J.*, **24**, 2224–2233.
14. Miao,Z.H., Agama,K., Sordet,O., Povirk,L., Kohn,K.W. and Pommier,Y. (2006) Hereditary ataxia SCAN1 cells are defective for the repair of transcription-dependent topoisomerase I cleavage complexes. *DNA Repair*, **5**, 1489–1494.
15. Hirano,R., Interthal,H., Huang,C., Nakamura,T., Deguchi,K., Choi,K., Bhattacharjee,M.B., Arimura,K., Umehara,F., Izumo,S. *et al.* (2007) Spinocerebellar ataxia with axonal neuropathy: consequence of a Tdp1 recessive neomorphic mutation? *EMBO J.*, **26**, 4732–4743.
16. Katyal,S., el-Khamisy,S.F., Russell,H.R., Li,Y., Ju,L., Caldecott,K.W. and McKinnon,P.J. (2007) TDP1 facilitates chromosomal single-strand break repair in neurons and is neuroprotective in vivo. *EMBO J.*, **26**, 4720–4731.
17. Rideout,M.C., Raymond,A.C. and Burgin,A.B. Jr (2004) Design and synthesis of fluorescent substrates for human tyrosyl-DNA phosphodiesterase I. *Nucleic Acids Res.*, **32**, 4657–4664.
18. Antony,S., Marchand,C., Stephen,A.G., Thibaut,L., Agama,K.K., Fisher,R.J. and Pommier,Y. (2007) Novel high-throughput electrochemiluminescent assay for identification of human tyrosyl-DNA phosphodiesterase (Tdp1) inhibitors and characterization of furamidine (NSC 305831) as an inhibitor of Tdp1. *Nucleic Acids Res.*, **35**, 4474–4484.
19. Marchand,C., Lea,W.A., Jadhav,A., Dexheimer,T.S., Austin,C.P., Inglese,J., Pommier,Y. and Simeonov,A. (2009) Identification of phosphotyrosine mimetic inhibitors of human tyrosyl-DNA phosphodiesterase I by a novel AlphaScreen high-throughput assay. *Mol. Cancer Ther.*, **8**, 240–248.
20. Nitiss,K.C., Malik,M., He,X., White,S.W. and Nitiss,J.L. (2006) Tyrosyl-DNA phosphodiesterase (Tdp1) participates in the repair of Top2-mediated DNA damage. *Proc. Natl Acad Sci. USA*, **103**, 8953–8958.
21. Barthelmes,H.U., Habermeyer,M., Christensen,M.O., Mielke,C., Interthal,H., Pouliot,J.J., Boege,F. and Marko,D. (2004) TDP1 overexpression in human cells counteracts DNA damage mediated by topoisomerases I and II. *J. Biol. Chem.*, **279**, 55618–55625.
22. He,X., van Waardenburg,R.C., Babaoglu,K., Price,A.C., Nitiss,K.C., Nitiss,J.L., Bjornsti,M.A. and White,S.W. (2007) Mutation of a conserved active site residue converts tyrosyl-DNA phosphodiesterase I into a DNA topoisomerase I-dependent poison. *J. Mol. Biol.*, **372**, 1070–1081.
23. Davies,D.R., Interthal,H., Champoux,J.J. and Hol,W.G. (2002) The crystal structure of human tyrosyl-DNA phosphodiesterase, Tdp1. *Structure*, **10**, 237–248.
24. Fisher,R.J., Fivash,M.J., Stephen,A.G., Hagan,N.A., Shenoy,S.R., Medaglia,M.V., Smith,L.R., Worthy,K.M., Simpson,J.T., Shoemaker,R. *et al.* (2006) Complex interactions of HIV-1 nucleocapsid protein with oligonucleotides. *Nucleic Acids Res.*, **34**, 472–484.
25. Lakowicz,J.R. (1999) *Principles of Fluorescence Spectroscopy*, 2nd edn. Springer-Verlag, New York.
26. Crockett,A.O. and Wittwer,C.T. (2001) Fluorescein-labeled oligonucleotides for real-time pcr: using the inherent quenching of deoxyguanosine nucleotides. *Anal. Biochem.*, **290**, 89–97.
27. Nazarenko,I., Pires,R., Lowe,B., Obaidy,M. and Rashtchian,A. (2002) Effect of primary and secondary structure of oligodeoxyribonucleotides on the fluorescent properties of conjugated dyes. *Nucleic Acids Res.*, **30**, 2089–2195.
28. Hergenrother,P.J., Haas,M.K. and Martin,S.F. (1997) Chromogenic assay for phospholipase D from Streptomyces chromofuscus: application to the evaluation of substrate analogs. *Lipids*, **32**, 783–788.
29. Sasnauskas,G., Connolly,B.A., Halford,S.E. and Siksnys,V. (2007) Site-specific DNA transesterification catalyzed by a restriction enzyme. *Proc. Natl Acad. Sci. USA*, **104**, 2115–2120.
30. Pouliot,J.J., Yao,K.C., Robertson,C.A. and Nash,H.A. (1999) Yeast gene for a Tyr-DNA phosphodiesterase that repairs topoisomerase I complexes. *Science*, **286**, 552–555.
31. Davies,D.R., Interthal,H., Champoux,J.J. and Hol,W.G. (2003) Crystal structure of a transition state mimic for Tdp1 assembled from vanadate, DNA, and a topoisomerase I-derived peptide. *Chem. Biol.*, **10**, 139–147.
32. Redinbo,M.R., Stewart,L., Kuhn,P., Champoux,J.J. and Hol,W.G. (1998) Crystal structures of human topoisomerase I in covalent and noncovalent complexes with DNA. *Science*, **279**, 1504–1513.
33. Pommier,Y., Barcelo,J., Rao,V.A., Sordet,O., Jobson,A.G., Thibaut,L., Miao,Z., Seiler,J., Zhang,H., Marchand,C. *et al.* (2006) Repair of topoisomerase I-mediated DNA damage. *Prog. Nucleic Acid Res. Mol. Biol.*, **81**, 179–229.
34. Nitiss,J.L. (2009) Targeting DNA topoisomerase II in cancer chemotherapy. *Nat. Rev. Cancer*, **9**, 338–350.
35. Cortes Ledesma,F., El Khamisy,S.F., Zuma,M.C., Osborn,K. and Caldecott,K.W. (2009) A human 5′-tyrosyl DNA phosphodiesterase that repairs topoisomerase-mediated DNA damage. *Nature*, **461**, 674–678.